

# Improved Memory Event-Triggered Load Frequency Control in Multi-Area Power System with Renewable Energy

Xinxin Lv, *Member, IEEE* Feng Qiao, *Member, IEEE* Yonghui Sun, *Member, IEEE*, Venkata Dinavahi, *Fellow, IEEE*, Peter Xiaoping Liu, *Fellow, IEEE*

**Abstract**—To mitigate the data transmission burden, an new memory event-trigger scheme is developed for the load frequency control (LFC) of multi-area networked power systems with the integration of various new energy sources.  $H_\infty$  stability criteria under less conservative conditions are established by utilizing an improved Lyapunov stability theory and a second-order Bessel-Legendre (B-L) inequality for the LFC power system using the presented memory event-trigger scheme. Simulation on a two-area LFC system and IEEE-39 bus station test system are performed to validate the proposed method.

**Index Terms**—Load frequency control, improved memory event-trigger, renewable energy.

## I. INTRODUCTION

LOAD frequency control (LFC) is crucial since it is responsible for ensuring stable power frequency and power exchange between areas for multi-area power system [1], [2]. Nowadays, digital equipment is increasingly replacing continuous-time equipment. It is possible to efficiently conserve communication resources by transmitting fewer data to have the required control effect [3]. Therefore, the event-trigger scheme is adopted in modern power systems to achieve expected goal of saving the occupancy of communication channel [4]. In an event-trigger scheme, the event generator will only release the data packet signal while the preset event-trigger conditions are satisfied [5]–[7]. In general, there are two main types of event-trigger schemes: continuous event-trigger scheme and discrete event-trigger scheme. Besides, there are some improved event-trigger schemes [8], [9]. Hence, research into the LFC power system is required, particularly in introducing an improved event-trigger scheme.

This work was supported in part by the Science Foundation of Zhejiang Sci-Tech University under Grant 21022311-Y, General Projects of Zhejiang Provincial Department of Education under Grant Y202250499, National Natural Science Foundation of China under Grant 61673161, in part by the Natural Science and Engineering Research Council (NSERC) of Canada. (corresponding author: Xinxin Lv.)

X. Lv, and F. Qiao are with the School of Information Science and Engineering, Zhejiang Sci-tech University, Hangzhou 310000, China (e-mail: xinxinlvhuc@163.com; ervingqf@163.com).

Y. Sun is with the College of Energy and Electrical Engineering, Hohai University, Nanjing 210098, China (e-mail: sunyonghui168@gmail.com).

V. Dinavahi is with the Department of Electrical and Computer Engineering, University of Alberta, Edmonton, Alberta T6G 2V4, Canada (e-mail: dinavahi@ualberta.ca).

P. X. Liu is with the Department of Systems and Computer Engineering, Carleton University, Ottawa, ON K1S 5B6, Canada (e-mail: xpliu@sce.carleton.ca).

Many researchers have paid attention to the improved event-trigger scheme in power systems. At first, the traditional event-trigger scheme is applied in power system [10], [11]. Liu et. al utilizes the event-triggered LFC for multi-area power systems [12]. The event-trigger scheme for power systems with communication delays is investigated to reduce the amount of data transmission in [13]. In an event-trigger scheme, the trigger performance is related to the threshold parameter. However, for the traditional event-trigger scheme, the trigger threshold needs to be preset, limiting the performance of the scheme. Then, an adaptive scheme with adaptive event-trigger communication scheme is studied in power system. The adaptive event-triggering  $H_\infty$  LFC for power systems is investigated in [14]. Moreover, adaptive event-triggered sliding mode control is utilized in multi-area power systems [15]. However, when the system is at a peak or trough, the burden of data sampling is very heavy in order to shorten the control time and achieve synchronization, and this is expected to be alleviated by advanced techniques.

With the deepening of research on event-trigger schemes, the memory event-trigger scheme is applied in power system. A memory event-trigger  $H_\infty$  LFC of a multi-area power system with transmission time delay is proposed in [16]. Mu et. al apply the memory event-trigger power system with a fuzzy model [17]. The memory-based event-triggering  $H_\infty$  LFC for power systems under deception attacks is built in [18]. For the memory event-triggered scheme, the trigger criteria are determined by several recently released signals and current trigger data; thus, the event-trigger scheme can obtain better trigger performance. However, the amount of data storage and computation in memory event-trigger scheme is increased, owing to some released data packets being saved in storage areas. Therefore, improving the memory event-trigger scheme is the motivation for this brief.

Motivated by the challenges influx of various network information into power systems, a novel memory event-triggered LFC is presented in this brief. The main contributions of this work can be summarized as follows: Considering the higher percentage of renewable energy resources within the power system, a multi-area LFC power system with both wind power and energy storage is studied. To reduce the burden of mass information transmission, a novel memory event-trigger scheme is developed. An improved Lyapunov function and second-order Bessel-Legendre (B-L) inequality are used to build the stability criteria with less conservation.

The remaining sections of this brief are structured as follows: Section II builds the model of novel memory event-triggered LFC power system with wind energy and energy storage units. In Section III, the stability of the designed multi-area LFC power system based on linear matrix inequality (LMI) is discussed. Section IV presents the simulation results and comparative analysis. Finally, Section V concludes the brief.

## II. PROBLEM STATEMENT

### A. Load frequency control system modelling

Considering the small fluctuations of load, the dynamic model of the multi-area power system LFC can be expressed as the following equation (1). Then the investigated multi-area LFC flow is described in Fig. 1. The parameters of the  $i$ -th control area are represented in Table I.

$$\begin{cases} \dot{x}(t) = Ax(t) + Bu(t) + F\omega(t) \\ y(t) = Cx(t) \end{cases} \quad (1)$$

where  $x_i(t) = [ \Delta f_i \quad \Delta P_{mi} \quad \Delta P_{vi} \quad \Delta P_{windi} \quad \Delta P_{Bi} \quad \int ACE_i \quad \Delta P_{tie-i} ]^T$ ,

$$x(t) = [ x_1^T(t) \quad x_2^T(t) \quad x_3^T(t) \quad \dots \quad x_n^T(t) ]^T,$$

$$u(t) = [ u_1^T(t) \quad u_2^T(t) \quad u_3^T(t) \quad \dots \quad u_n^T(t) ]^T,$$

$$\omega_i(t) = [ \Delta P_{di} \quad \Delta \Phi_{windi} ]^T,$$

$$A_{ij} = [(7, 1) = -2\pi T_{ij}], y_i(t) = [ ACE_i \quad \int ACE_i ]^T,$$

$$\omega(t) = [ \omega_1^T(t) \quad \omega_2^T(t) \quad \omega_3^T(t) \quad \dots \quad \omega_n^T(t) ]^T,$$

$$y(t) = [ y_1^T(t) \quad y_2^T(t) \quad y_3^T(t) \quad \dots \quad y_n^T(t) ]^T,$$

$$B_i = \begin{bmatrix} 0 & 0 & (\frac{1}{T_{gi}})^T & 0 & 0 & 0 & 0 \end{bmatrix}^T,$$

$$B = \text{diag}\{B_1, \dots, B_n\}, C = \text{diag}\{C_1, \dots, C_n\}$$

$$A_{ii} = \begin{bmatrix} (1, 1) = \frac{-D}{M_i}, (1, 2) = \frac{1}{M_i}, (1, 4) = \frac{1}{M_i}, \\ (1, 5) = \frac{1}{M_i}, (1, 7) = \frac{-1}{M_i}, (2, 2) = \frac{-1}{T_{chi}}, \\ (2, 3) = \frac{1}{T_{chi}}, (3, 1) = \frac{-1}{RT_{gi}}, (3, 3) = \frac{-1}{T_{gi}}, \\ (4, 4) = \frac{-1}{T_{wi}}, (5, 1) = \frac{1}{T_{ESi}}, \\ (5, 5) = \frac{-1}{T_{ESi}}, (6, 1) = \beta_i, \\ (6, 6) = 1, (7, 1) = 2\pi \sum_{j=1, j \neq i}^n T_{ij} \end{bmatrix},$$

$$A = \begin{bmatrix} A_{11} & \dots & A_{1n} \\ \vdots & \ddots & \vdots \\ A_{n1} & \dots & A_{nn} \end{bmatrix}, F = \text{diag}\{F_1, \dots, F_n\},$$

$$C_i = \begin{bmatrix} \beta_i & 0 & 0 & 0 & 0 & 0 & 1 \\ 0 & 0 & 0 & 0 & 0 & 1 & 0 \end{bmatrix},$$

$$F_i = \begin{bmatrix} \frac{-1}{M_i^T} & 0 & 0 & 0 & 0 & 0 & 0 \\ 0 & 0 & 0 & \frac{1}{T_{wi}} & 0 & 0 & 0 \end{bmatrix}^T$$

The area control error (ACE) signal can be written as

$$ACE_i = \beta_i \Delta f_i + \Delta P_{tie-i} \quad (2)$$

### B. Novel memory event-trigger scheme for LFC power system

To relieve the information transmission burden of multi-area power system, a improved event-trigger scheme is employed in this brief. Compared with traditional event-trigger schemes, the improved memory event-trigger scheme can store a recent

TABLE I  
NOTATIONS

Symbol	Quantity
$\Delta P_{di}$	Load deviation
$\Delta P_{mi}$	Generator mechanical output deviation
$\Delta P_{vi}$	Valve position deviation
$\Delta P_{windi}$	Output power fluctuation of the wind turbine generator
$\Delta P_{Bi}$	Output power fluctuation of the battery
$\Delta P_{tie-i}$	Tie-line power deviation
$\Delta f_i$	Frequency deviation
$\Delta \Phi_{windi}$	Wind power deviation
$M_i$	Moment of inertia
$D_i$	Generator damping coefficient
$T_{gi}$	Time constant of the governor
$T_{chi}$	Time constant of the turbine
$T_{wi}$	Time constant of the wind turbine
$T_{ESi}$	Time constant of the battery
$R_i$	Speed drop
$\beta_i$	Frequency bias factor
$T_{ij}$	Tie-line synchronizing coefficient
$ACE_i$	Area control error

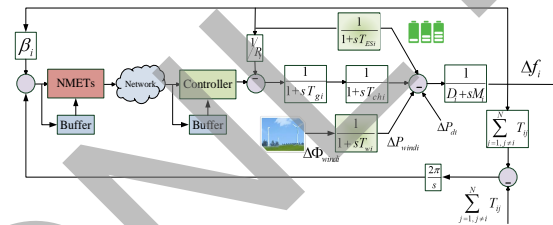


Fig. 1. Transfer function model of multi-area power system.

triggering threshold, which is used to adjust the event-trigger condition. For traditional event-trigger schemes, signal packets can be delivered if the designed trigger threshold can be satisfied. The traditional event-trigger criterion is designed as  $[x(t_k h + j h) - x(t_k h)]^T \Phi [x(t_k h + j h) - x(t_k h)] \geq \lambda x^T(t_k h) \Phi x(t_k h)$

where  $\Phi$  is an unknown positive matrix;  $\lambda$  denotes the triggering threshold which needs to be preset.

Unlike the traditional event-trigger scheme, the proposed memory event-trigger scheme utilizes not only the changes between the current sampling moment data and the last released information but also the previous trigger threshold. Therefore, the designed novel memory event-trigger scheme can be described as

$$\begin{aligned} [x(t_k h + j h) - x(t_k h)]^T \Phi [x(t_k h + j h) - x(t_k h)] \\ \geq \lambda(t_k h) x^T(t_k h) \Phi x(t_k h) \end{aligned} \quad (3)$$

where

$$\lambda(t_k h) = \begin{cases} \lambda(t_{k-1} h) & \text{if } \frac{\|x(t_{k-1} h) - x(t_k h)\|}{x(t_k h)} > c \\ a\lambda(t_{k-1} h) + b\lambda(t_{k-2} h) & \text{if } \frac{\|x(t_{k-1} h) - x(t_k h)\|}{x(t_k h)} \leq c \end{cases},$$

$a + b = 1$ , and  $0 \leq c \leq 1$  is a unknown positive matrix.

Define:

$$\tau(t) = \begin{cases} t - t_k h, & t \in \Omega_{k,n}^1 \\ t - t_k h - m h, & t \in \Omega_{k,n}^2 \\ t - t_k h - K h, & t \in \Omega_{k,n}^3 \end{cases} \quad (4)$$

where  $\Omega_{k,n}^1 = [t_k h + \tau_k, (t_k + 1)h + \tau_k]$ ,  $\Omega_{k,n}^2 = \cup_{m=1}^{K-1} [t_k h + m h + \tau_k, t_k h + (m-1)h + \tau_k]$ ,  $\Omega_{k,n}^3 = [t_k h + K h + \tau_k, t_{k+1} h + \tau_{k+1}]$

The controller input can be described as:

$$y(t_{k,n} h) = C e_{k,n}(t) + C x(t - \tau_{k,n}(t)) \quad (5)$$

where

$$e(t) = \begin{cases} 0, & k \in \Omega_{k,n}^1 \\ x(t_{k,n}h) - x(t_{k,n}h + mh), & k \in \Omega_{k,n}^2 \\ x(t_{k,n}h) - x(t_{k,n}h + jh), & k \in \Omega_{k,n}^3 \end{cases}$$

and  $j = \sup\{m \in N | t_k h + mh < t_{k+1} h, m = 1, 2, \dots\}$ ,  $\tau_M = \max(\tau_{k,n}(t))$ .

Therefore, the designed novel memory event-trigger condition can be described as

$$e^T(t)\Phi e(t) \geq \lambda(t_k h)x^T(t_k h)\Phi x(t_k h) \quad (6)$$

Then, the studied LFC power system model can be revised as:

$$\dot{x}(t) = Ax(t) + BKCe(t) + BKCx(t - \tau(t)) + F\omega(t) \quad (7)$$

*Remark 1:* For the designed trigger scheme, the current sampling moment data, along with the last released information and the previous trigger threshold, are utilized to determine whether the current sampling moment data can be transmitted. Compared with traditional event-trigger schemes, the designed scheme can better release redundant information with the adaptively trigger threshold. In addition, compared with memory event-trigger scheme, the proposed scheme does not require calculating the previous triggering condition; it only stores the previous trigger threshold, reducing the computational burden. Therefore, the applied novel memory event-trigger scheme possesses excellent performance.

### III. STABILITY ANALYSIS OF MEMORY EVENT-TRIGGERED LFC

Applying the proposed novel memory event-trigger scheme, the stability and stabilization criteria of the multi-area LFC model will be derived. Then, an improved Lyapunov function and integral inequality with an auxiliary function are employed to build the stability criteria in the following.

*Theorem 1:* For given constant  $\lambda_m$ ,  $\tau_M$ ,  $\hat{\tau}$ , if there exists positive definite matrices  $P$ ,  $Q_1$ ,  $Q_2$ ,  $R_1$ ,  $R_2$ ,  $S_1$ ,  $S_2$ ,  $\Phi$ , appropriate dimensions  $T_{11}$ ,  $T_{12}$ ,  $T_{13}$ ,  $T_{21}$ ,  $T_{22}$ ,  $T_{23}$ ,  $T_{31}$ ,  $T_{32}$ ,  $T_{33}$ , and the following LMIs hold, the studied LFC model (1) with  $\omega(k) = 0$  is asymptotically stable.

$$\Pi_2 = \Pi_1 + \hat{H}_2 \tilde{\varphi}_1 \hat{H}_2^T + \varphi_3 + \varphi_4 + 2P\chi_1 + \chi_1 v_2 \chi_1^T < 0 \quad (8)$$

$$\tilde{\varphi}_2 = \begin{bmatrix} \varphi_1 + \tilde{S}_1 & * \\ T_1 & \varphi_1 + \tilde{S}_2 \end{bmatrix} > 0 \quad (9)$$

where  $\Pi_1 = e_1 v_1 e_1^T - e_2 \Phi e_2^T - e_3 Q_1 e_3^T - e_4 v_3 e_4^T$ ,  $v_1 = Q_1 + \tau_M R_2$ ,  $v_2 = \tau_M^2 R_1 + \frac{\tau_M^2}{2} S_1 + \frac{\tau_M^2}{2} S_2$ ,  $v_3 = (1 - \hat{\tau}(t))Q_2 - \lambda(t_k h)\Phi$ ,  $\chi_1 = Ae_1 + BKCe_2 + BKCe_4$ ,  $\varphi_1 = \text{diag}\{R_1, 3R_1, 5R_1\}$ ,  $\hat{H}_2 = [H_1 \ H_2]$ ,  $\varphi_3 = \text{diag}\{-2S_1, -4S_1, -2S_1, -4S_1\}$ ,  $\varphi_4 = \text{diag}\{-2S_2, -4S_2, -2S_2, -4S_2\}$ ,  $H_1 = [e_1 - e_4 \ e_1 + e_4 - 2e_5 \ e_1 - e_4 - 6e_6]$ ,  $H_2 = [e_4 - e_3 \ e_3 + e_4 - 2e_7 \ e_4 - e_3 - 6e_8]$ ,  $H_3 = [e_1 - e_5 \ e_1 - e_5 - 3e_6 \ e_4 - e_7 \ e_4 - e_7 - 3e_8]$ ,  $H_4 = [e_5 - e_4 \ e_4 - e_5 + 3e_6 \ e_7 - e_3 \ e_3 - e_7 + 3e_8]$ ,  $\tilde{S}_1 = \text{diag}\{S_1, 3S_1, 5S_1\}$ ,  $\tilde{S}_2 = \text{diag}\{S_2, 3S_2, 5S_2\}$ ,

$$\tilde{\varphi}_1 = \begin{bmatrix} \varphi_1 & * \\ T_1 & \varphi_1 \end{bmatrix}, \tilde{\varphi}_2 = \begin{bmatrix} \varphi_1 + \tilde{S}_1 & * \\ T_1 & \varphi_1 + \tilde{S}_2 \end{bmatrix} > 0,$$

$$T_1 = \begin{bmatrix} T_{11} & T_{12} & T_{13} \\ T_{21} & T_{22} & T_{23} \\ T_{31} & T_{32} & T_{33} \end{bmatrix}, e_j = [\underbrace{0 \dots 0}_{j-1}, 1, \underbrace{0 \dots 0}_{8-j}], (j = 1, \dots, 8)$$

*Proof:* Build the following Lyapunov function:

$$V(t) = x^T(t)Px(t) + \int_{t-\tau_M}^t x^T(s)Q_1x(s)ds + \int_{t-\tau(t)}^t x^T(s)Q_2x(s)ds + \tau_M \int_{-\tau_M}^0 \int_{t+\alpha}^t \dot{x}^T(s)R_1\dot{x}(s)dsd\alpha + \int_{-\tau_M}^0 \int_{t+\alpha}^t x^T(s)R_2x(s)dsd\alpha + \int_{-\tau_M}^0 \int_{\beta}^0 \int_{t+\alpha}^t \dot{x}^T(s)S_1\dot{x}(s)dsd\alpha d\beta + \int_{-\tau_M}^0 \int_{-\tau_M}^{\beta} \int_{t+\alpha}^t \dot{x}^T(s)S_2\dot{x}(s)dsd\alpha d\beta$$

Calculating the derivative of  $V(t)$  along the trajectory of (1) with  $\omega(t) = 0$  yields:

$$\begin{aligned} \Delta V(t) &= 2\dot{x}^T(t)Px(t) + x^T(t)(Q_1 + Q_2 + \tau_M R_2)x(t) \\ &\quad - x^T(t-\tau_M)Q_1x(t-\tau_M) - (1-\dot{\tau}(t))x^T(t-\tau(t))Q_2x(t-\tau(t)) \\ &\quad + \dot{x}^T(t)(\tau_M^2 R_1 + \frac{\tau_M^2}{2} S_1 + \frac{\tau_M^2}{2} S_2)\dot{x}(t) \\ &\quad - \tau_M \int_{t-\tau_M}^t \dot{x}^T(\alpha)R_1\dot{x}(\alpha)d\alpha - \int_{t-\tau(t)}^t \dot{x}^T(\alpha)R_2x(\alpha)d\alpha \\ &\quad - \tau(t) \int_{t-\tau(t)}^t \dot{x}^T(s)S_2\dot{x}(s)ds \\ &\quad - \int_{-\tau(t)}^0 \int_{t+\alpha}^t \dot{x}^T(s)S_1\dot{x}(s)dsd\alpha \\ &\quad - \int_{-\tau_M}^{-\tau(t)} \int_{t+\alpha}^{t-\tau(t)} \dot{x}^T(s)S_1\dot{x}(s)dsd\alpha \\ &\quad - (\tau_M - \tau(t)) \int_{t-\tau(t)}^t \dot{x}^T(\alpha)S_1\dot{x}(\alpha)d\alpha \\ &\quad - \int_{-\tau(t)}^0 \int_{t-\tau(t)}^{t+\alpha} \dot{x}^T(s)S_2\dot{x}(s)dsd\alpha \\ &\quad - \int_{-\tau_M}^{-\tau(t)} \int_{t-\tau_M}^{t+\alpha} \dot{x}^T(s)S_2\dot{x}(s)dsd\alpha \end{aligned}$$

Set the augmented vector as follows:

$$\xi(t) = [x(t) \ e(t) \ x(t - \tau_M) \ x(t - \tau(t)) \ \frac{1}{\tau(t)} \int_{-\tau(t)}^0 x(t + \alpha)d\alpha \ \frac{1}{\tau(t)} \int_{-\tau(t)}^0 \lambda_{-\tau(t)}(\alpha)x(t + \alpha)d\alpha \ \frac{1}{\tau_M - \tau(t)} \int_{-\tau_M}^{-\tau(t)} x(t + \alpha)d\alpha \ \frac{1}{\tau_M - \tau(t)} \int_{-\tau_M}^{-\tau(t)} \lambda_{-\tau(t)}(\alpha)x(t + \alpha)d\alpha]$$

Then, the following inequality can be derived as

$$\Delta V(t) \leq \xi(t)\Pi_1\xi^T(t) + 2\dot{x}(t)Px^T(t) + \dot{x}(t)v_2\dot{x}^T(t) + \Delta\tilde{V}_1(t) + \Delta\tilde{V}_2(t) + \Delta\tilde{V}_3(t) \quad (10)$$

where  $\Delta\tilde{V}_1(t) = -\tau_M \int_{t-\tau_M}^t \dot{x}(s)R_1\dot{x}^T(s)ds - (\tau_M - \dot{\tau}(t)) \int_{t-\tau(t)}^t \dot{x}(s)S_1\dot{x}^T(s)ds - \dot{\tau}(t) \int_{t-\tau(t)}^t \dot{x}(s)S_2\dot{x}^T(s)ds$

$$\Delta\tilde{V}_2(t) = -\int_{-\tau(t)}^0 \int_{t+\alpha}^t \dot{x}(s)S_1\dot{x}^T(s)dsd\alpha$$

$$- \int_{-\tau_M}^{-\tau(t)} \int_{t+\alpha}^{t-\tau(t)} \dot{x}(s)S_1\dot{x}^T(s)dsd\alpha$$

$$\Delta\tilde{V}_3(t) = -\int_{-\tau(t)}^0 \int_{t-\tau(t)}^{t+\alpha} \dot{x}(s)S_2\dot{x}^T(s)dsd\alpha$$

$$- \int_{-\tau_M}^{-\tau(t)} \int_{t-\tau_M}^{t+\alpha} \dot{x}(s)S_2\dot{x}^T(s)dsd\alpha$$

In the following, the second-order B-L inequality in [19] can be applied for  $\Delta\tilde{V}_1(t)$ . Define  $\frac{1}{\iota} = \frac{\tau(t)}{\tau_M}$  and  $\frac{1}{\kappa} = \frac{\tau_M - \tau(t)}{\tau_M}$ , and applying it in  $\Delta\tilde{V}_1(t)$ . Then, double integral inequality in [20] can be utilized for  $\Delta\tilde{V}_2(t)$  and  $\Delta\tilde{V}_3(t)$ .

Therefore, if  $\tilde{\varphi}_2 > 0$  can be satisfied, the following inequality can be yielded:

$$\begin{aligned} \Delta V(t) &\leq \xi(t)\Pi_1\xi^T(t) + 2\dot{x}(t)Px^T(t) + \dot{x}(t)v_2\dot{x}^T(t) \\ &\quad + \Delta\tilde{V}_1(t) + \Delta\tilde{V}_2(t) + \Delta\tilde{V}_3(t) \\ &\leq \xi(t)\Pi_2\xi^T(t) \end{aligned} \quad (11)$$

Thus, by utilizing the Lemma 1 in [20] the condition (8) can be derived. With a condition that  $\omega(k) = 0$ , if (8) and (9) are satisfied, there exists a sufficiently small scalar  $c \in (0, 1]$ , such

that  $\Delta V(k) < -c\|\xi_1(t)\|^2 < 0$  can be procured. As a result, the system (1) with  $\omega(k) = 0$  is asymptotically stable.

*Remark 2:* The improved Lyapunov function with the triple integral term in  $V(t)$  is applied in this section. Then, the maximum time delay  $\tau_M$  and  $\hat{\tau}$  are considered in this theorem. In addition, a second-order B-L inequality is applied in  $\Delta \tilde{V}_1(t)$  which can provide tighter upper bounds than those acquired by [20].

Following that,  $H_\infty$  stability criterion of the multi-area LFC model (1) will be developed.

*Theorem 2:* For given constant  $\lambda_m$ ,  $\tau_M$ ,  $\hat{\tau}$ , if there exist positive definite matrices  $P$ ,  $Q_1$ ,  $Q_2$ ,  $R_1$ ,  $R_2$ ,  $S_1$ ,  $S_2$ ,  $\Phi$ , appropriate dimensions  $T_{11}$ ,  $T_{12}$ ,  $T_{13}$ ,  $T_{21}$ ,  $T_{22}$ ,  $T_{23}$ ,  $T_{31}$ ,  $T_{32}$ ,  $T_{33}$ , and the following LMIs hold, the multi-area LFC model (1) is asymptotically stable with an  $H_\infty$  norm bound  $\gamma$ .

$$\tilde{\varphi}_2 > 0$$

$$\begin{aligned} \Pi'_2 &= \Pi_1 + \hat{H}_2 \tilde{\varphi}_1 \hat{H}_2^T + \varphi_3 + \varphi_4 + 2P\chi'_1 + \chi'_1 v_2 \chi'^T_1 \\ &\quad - \gamma^2 e_{10}^T e_{10} + e_1^T C^T C e_1 < 0 \end{aligned} \quad (12)$$

where  $\chi'_1 = Ae_1 + BKCe_2 + BKCe_4 + Fe_9$ ,  $e_j = [0, \dots, 0, 1, 0, \dots, 0]$ , ( $j = 1, \dots, 9$ )

For prescribed attenuation level  $\gamma > 0$ , taking the disturbance  $\omega(t)$  into account, the cost function  $J$  is considered as

$$J = \int_0^\infty y^T(t)y(t) - \gamma^2 \omega^T(t)\omega(t) dt \quad (13)$$

Setting the augmented vector as  $\xi'(t) = [\xi(t) \ \omega(t)]^T$ .

*Remark 3:* The sufficient stability condition of the multi-area LFC model (1) is provided in Theorem 1 and Theorem 2. To design the controller gain, recalling (12) and employing Lemma 1 in [20], the following inequality can be obtained:

$$\begin{bmatrix} \Phi''_1 & * \\ \Phi_{21} & \Phi_{22} \end{bmatrix} < 0 \quad (14)$$

where  $\Phi''_1 = \Pi_1 + \hat{H}_2 \tilde{\varphi}_1 \hat{H}_2^T + \varphi_3 + \varphi_4 - \gamma^2 e_{10}^T e_{10} + e_1^T C^T C e_1$ ,  $\Phi_{21} = \Phi_{21} = [P\chi''_2 \ \tau_M \chi''_2 \ \tau_M / \sqrt{2} \chi''_1 \ \tau_M / \sqrt{2} \chi''_1]^T$ ,  $\Phi_{22} = \text{diag}(-P^{-1}, -R_1^{-1}, -S_1^{-1}, -S_1^{-1})$

Pre-multiplying and post-multiplying both sides of (14) with  $\text{diag}\{I, \underbrace{\dots}_9, I, P, P, P\}$ , and utilizing the fact that  $Z < 0$ ,  $Y^T = Y$ , then  $Y^T Z Y \leq -2Y - Z^{-1}$  can be obtained, and  $\Pi'_2 < 0$  can be further converted. Therefore, the theorem is proved and the controller gain is  $\tilde{K} = PK$ .

#### IV. CASE STUDY AND DISCUSSION

A two-area interconnected power system and IEEE-39 bus station test system are applied in this section to validate the proposed novel memory event-trigger scheme.

Case A: Two-area LFC power system with improved memory event-trigger scheme

Consider a two-area LFC power system with wind farms and energy storage units as shown in [20]. The detailed parameters are in [20]. To analyze the designed memory event-trigger scheme performance for two-area LFC power system, the improved memory event-trigger scheme with  $c = 0.2$  and  $c = 0.6$  are explored in this case, respectively.

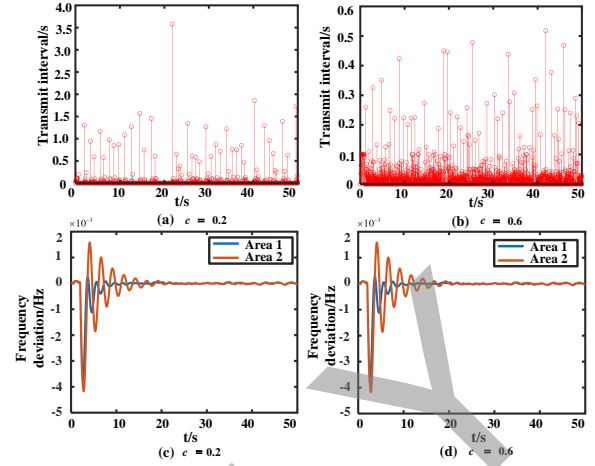


Fig. 2. Results of  $c = 0.2$  and  $c = 0.6$ : (a) Release, (b) Frequency deviations of Area 2, (c) ACE of Area 1, (d) ACE of Area 2.

To evaluate the designed improved memory event-trigger scheme performance, release time instants and intervals with  $c = 0.2$  and  $c = 0.6$  are depicted in Fig. 2(a), (b). It can be observed that less information is transmitted in the second situation with  $c = 0.2$ , compared with the first situation with  $c = 0.6$ . The proposed improved memory event-trigger scheme can eliminate unnecessary information exchange and relieve the transmission burden for LFC power system.

To scrutinize the LFC scheme performance under developed novel memory event-trigger scheme, frequency deviation changes and ACE changes are manifest in Fig. 2(c), (d). When external disturbances occur, the designed power frequency deviation changes and ACE changes can go back to the preset value immediately. Therefore, the designed LFC with novel memory event-trigger scheme can adjust frequency to near-stable conditions effectively, and the designed memory event-trigger scheme can reduce the redundancy of signal data transmission.

Case B: The modified IEEE-39 bus test power system with improved memory event-trigger scheme

To verify the performance of the proposed improved memory event-trigger scheme in power system, an IEEE-39 bus model is built using MATLAB/Simulink, as shown in Fig. 3. The system is divided into three control areas, with Gen3, Gen7 and Gen9 as the selected generator in Area 1, Area 2 and Area 3, respectively. Moreover, the traditional event-trigger scheme, adaptive event-trigger scheme and the improved memory event-trigger scheme is utilized in Area 1, Area 2 and Area 3, respectively.

At  $t = 20s$ ,  $t = 50s$  and  $t = 80s$ , perturbation is added to Bus 8, Bus 16 and Bus 3, respectively. At this time, the response, trigger interval and trigger time in three areas are shown in Fig. 4.

As can be seen from Fig. 4, the frequency deviation in three areas converges to a steady state within a short period of time. At the moment of the perturbation, the system performance needs a large amount of data for improvement, the event-trigger scheme transmits a large amount of data at

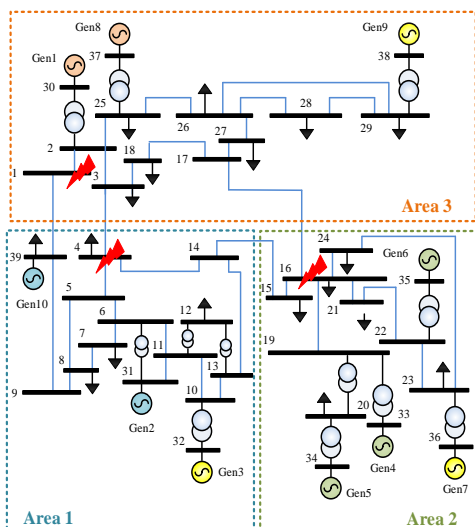


Fig. 3. IEEE-39 bus test system.

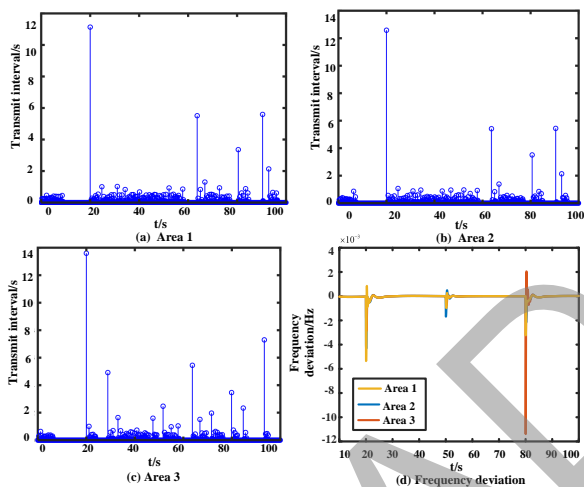


Fig. 4. Transmit interval and frequency deviation.

this time. However, the least amount of data is transmitted in Area 3 under designed improved memory event-trigger scheme. Therefore, the proposed improved memory event-trigger scheme in this brief has a better performance in reducing the amount of redundant information transmission.

### V. CONCLUSION

A new memory event-trigger scheme is developed for the load frequency control of power systems with renewable energy resources. An improved Lyapunov function and a second-order B-L inequality are applied to obtain the stability criteria with less conservatism. The simulation of two-area LFC power system and IEEE-39 bus test system are conducted to validate the proposed novel memory event-trigger scheme. In comparison with the traditional event-trigger scheme, the presented event-trigger scheme can significantly reduce redundant data transmission and there is no need to calculate the previous triggering condition.

### REFERENCES

- [1] Y. Wang, Y. Wang, Y. Sun, V. Dinavahi, J. Liang and K. Wang, "Resilient dynamic state estimation for multi-machine power system with partial missing measurements," *IEEE Trans. Power Syst.*, doi: 10.1109/TPWRS.2023.3287151, 2023.
- [2] X. Xie, Q. Zhou, D. Yue and H. Li, "Relaxed control design of discrete-time Takagi-sugeno fuzzy systems: An event-triggered real-time scheduling approach," *IEEE Trans. Syst. Man Cybern. Syst.*, vol. 48, no. 12, pp. 2251-2262, 2018.
- [3] S. Yan, Z. Gu, J. H. Park, X. Xie and C. Dou, "Probability-density-dependent load frequency control of power systems with random delays and cyber-attacks via circuitual implementation," *IEEE Trans. Smart Grid*, vol. 13, no. 6, pp. 4837-4847, 2022.
- [4] N. Zhang, Q. Sun, L. Yang and Y. Li, "Event-triggered distributed hybrid control scheme for the integrated energy system," *IEEE Trans. Industr. Inform.*, vol. 18, no. 2, pp. 835-846, 2022.
- [5] T. Li, D. Yang, X. Xie and H. Zhang, "Event-triggered control of nonlinear discrete-time system with unknown dynamics based on HDP( $\lambda$ )," *IEEE Trans. Cybern.*, vol. 52, no. 7, pp. 6046-6058, 2022.
- [6] X. Chu, Z. Liu, L. Mao, X. Jin, Z. Peng and G. Wen, "Robust event triggered control for lateral dynamics of intelligent vehicle with designable inter-event times," *IEEE Trans. Circuits Syst. II, Exp. Briefs*, vol. 69, no. 11, pp. 4349-4353, 2022.
- [7] K. Liu and Z. Ji, "Dynamic event-triggered consensus of general linear multi-agent systems with adaptive strategy," *IEEE Trans. Circuits Syst. II, Exp. Briefs*, vol. 69, no. 8, pp. 3440-3444, 2022.
- [8] M. Shahvali, M. Sistani and J. Askari, "Dynamic event-triggered control for a class of nonlinear fractional-order systems," *IEEE Trans. Circuits Syst. II, Exp. Briefs*, vol. 69, no. 4, pp. 2131-2135, 2022.
- [9] Z. Chen, B. Niu, Z. Zhao and L. Zhang and N. Xu, "Model-based adaptive event-triggered control of nonlinear continuous-time systems," *Appl. Math. Comput.*, vol. 408, pp. 126330, 2021.
- [10] Z. Wu, H. Mo, J. Xiong and M. Xie, "Adaptive event-triggered observer-based output feedback  $\mathcal{L}_\infty$  load frequency control for networked power systems," *IEEE Trans. Industr. Inform.*, vol. 16, no. 6, pp. 3952-3962, 2020.
- [11] P. Chen, D. Zhang, L. Yu and H. Yan, "Dynamic event-triggered output feedback control for load frequency control in power systems with multiple cyber attacks," *IEEE Trans. Syst., Man, Cybern., Syst.*, vol. 52, no. 10, pp. 6246-6258, 2022.
- [12] J. Liu, Y. Gu, L. Zha, Y. Liu and J. Cao, "Event-triggered  $H_\infty$  load frequency control for multiarea power systems under hybrid cyber attacks," *IEEE Trans. Syst., Man, Cybern., Syst.*, vol. 49, no. 8, pp. 1665-1678, 2019.
- [13] S. Wen, X. Yu, Z. Zeng and J. Wang, "Event-triggering load frequency control for multiarea power systems with communication delays," *IEEE Trans. Ind. Electron.*, vol. 63, no. 2, pp. 1308-1317, 2016.
- [14] C. Peng, J. Zhang and H. Yan, "Adaptive event-triggering  $H_\infty$  load frequency control for network-based power systems," *IEEE Trans. Ind. Electron.*, vol. 65, no. 2, pp. 1685-1694, 2018.
- [15] W. Qi, G. Zong and W. Zheng, "Adaptive event-triggered SMC for stochastic switching systems with semi-Markov process and application to boost converter circuit model," *IEEE Trans. Circuits Syst.*, vol. 68, no. 2, pp. 786-796, 2021.
- [16] S. Yan, Z. Gu and H. Ju, "Memory event-triggered  $H_\infty$  load frequency control of multi-area power systems with cyber-attacks and communication delays," *IEEE Trans. Netw. Sci. Eng.*, vol. 8, no. 2, pp. 1571-1583, 2021.
- [17] X. Mu, G. Zhou and L. Hua, "Memory-based event-triggered leader-following consensus for T-S fuzzy multi-agent systems subject to deception attacks," *J. Franklin Inst.*, vol. 359, no. 1, pp. 599-618, 2022.
- [18] E. Tian and C. Peng, "Memory-based event-triggering  $H_\infty$  load frequency control for power systems under deception attacks," *J. Franklin Inst.*, vol. 50, no. 11, pp. 4610-4618, 2022.
- [19] P. Park, W. Lee and S. Lee, "Auxiliary function-based integral inequalities for quadratic functions and their applications to time-delay systems," *J. Franklin Inst.*, vol. 352, pp. 1378-6304, 2022.
- [20] X. Lv, Y. Sun, W. Hu and V. Dinavahi, "Robust load frequency control for networked power system with renewable energy via fractional-order global sliding mode control," *IET Renew. Power Gener.*, vol. 15, no. 5, pp. 1046-1057, 2021.